

Alkylation, Cation Formation, and Insertion Reactions in Titanium Tris(ketimide) Complexes

M. João Ferreira,[†] Inês Matos,[†] José R. Ascenso,[†] M. Teresa Duarte,[†] M. Mercês Marques,[†] Claire Wilson,[‡] and Ana M. Martins^{*,†}

Centro de Química Estrutural, Instituto Superior Técnico, Av. Rovisco Pais, 1, 1049-001 Lisboa, Portugal, and School of Chemistry, University of Nottingham, Nottingham NG7 2RD, U.K.

Received June 26, 2006

Ti(N=C^tBu₂)₃Cl (**1**) reacts with TlPF₆ in acetonitrile to afford [Ti(N=C^tBu₂)₃(N≡CCH₃)]PF₆ (**2**), which proved to be unstable and decomposed at room temperature either in solution or in the solid state. Attempts to recrystallize **2** from a CH₂Cl₂/hexane mixture led to [Ti₃(N=C^tBu₂)₆(μ₂-F)₃(μ₃-F)₂][PF₆] (**3**). Treatment of **1** with LiMe and PhCH₂MgCl gave the compounds Ti(N=C^tBu₂)₃CH₂Ph (**4**) and Ti(N=C^tBu₂)₃Me (**5**), respectively. **4** was treated with B(C₆F₅)₃ to afford [Ti(N=C^tBu₂)₃(CH₂Ph)B(C₆F₅)₃] (**6**), which exists in solution as a mixture of two species, the zwitterion [Ti(N=C^tBu₂)₃][(μ-CH₂Ph)B(C₆F₅)₃] (**6A**) and the solvate cation [Ti(N=C^tBu₂)₃(Solv)][(CH₂Ph)B(C₆F₅)₃] (**6B**). Above 60 °C, C₆F₅ is transferred to the metal center and Ti(N=C^tBu₂)₃(C₆F₅) (**9**) forms. This compound participates in a dynamic process in solution involving Ti···F interactions. The fluxional process observed for **6** can be stopped upon addition of 1 equiv of C≡NMe_s, giving [Ti(N=C^tBu₂)₃(C≡NMe_s)][(CH₂Ph)B(C₆F₅)₃] (**7**). C≡NMe_s does not insert into Ti–N bonds, but it readily inserts into the Ti–C bond of Ti(N=C^tBu₂)₃(Me) (**5**) to afford [Ti(N=C^tBu₂)₃{η²-C(CH₃)=NMe_s}] (**8**).

Introduction

Preliminary work on early-transition-metal ketimide complexes emerged from nitrile reactivity studies, namely insertions into metal–carbon or metal–hydride bonds. The resulting ketimide ligands proved to be relatively inert toward nucleophilic and electrophilic reagents, being nevertheless susceptible to hydrolysis, leading to ketimines or ketones.¹ This robustness remained unexplored until recently, when ketimide ligands were investigated as supports of early-transition-metal complex reactivity. Compounds of the type Cp[′]Ti(N=C^tBu₂)Cl₂ (Cp[′] = Cp, Cp^{*}, Ind, C₅H₄^tBu), patented by Nova Chemicals,² have proven to be extremely active catalysts in ethylene,^{3–6} propylene,³ and 1-hexene^{4,5} homopolymerizations and show good activities in syndiospecific styrene homopolymerization.⁵ These complexes are also capable of copolymerizing ethylene with polar (10-undecen-1-ol³) and apolar monomers (1-hexene⁴ and styrene⁶). Particularly noteworthy is the ethylene–styrene copolymerization that was obtained in a living manner by Nomura et al.^{6,7} The cationic complexes [Cp[′]Ti(N=CR₁R₂)-Me]⁺, which are accepted as the active species in olefin polymerization catalysis, have been studied by Piers et al.^{8,9}

We have recently shown that the titanium tris(ketimide) complex Ti(N=C^tBu₂)₃Cl (**1**) is a good ethylene polymerization catalyst when activated by MAO.¹⁰ In this work we present further results involving titanium tris(ketimide) complexes, namely alkylation, cation generation, and stability, as well as insertion reactions, which are relevant to the behavior of tris(ketimide) compounds as olefin polymerization catalysts.

Results and Discussion

Scheme 1 presents all the new compounds discussed in this work.

Ti(N=C^tBu₂)₃Cl¹⁰ (**1**) reacts in acetonitrile with TlPF₆ to afford [Ti(N=C^tBu₂)₃(N≡CCH₃)]PF₆ (**2**) as a bright yellow solid. Salt formation was confirmed by the presence of the PF₆[−] ion, as attested by the doublet at −67.4 ppm in the ¹⁹F NMR spectrum and the septet at −138.7 ppm in the ³¹P NMR spectrum, both with ¹J_{PF} = 708.6 Hz, and the singlet at δ 1.98 ppm due to the coordinated CH₃CN proton resonance. This complex is not stable, however, decomposing at room temperature, as indicated by a dramatic color change from yellow to green. The decomposition process involves fluoride transfer to titanium, as suggested by the formation of [Ti₃(N=C^tBu₂)₆(μ₂-F)₃(μ₃-F)₂][PF₆] (**3**) while attempting to recrystallize **2** from a CH₂Cl₂/hexane solution, at −20 °C. The formation of **3** from complex **2** attests to the lability of the acetonitrile ligand and is suggestive of ion-pair contact between the very acidic titanium cation and the PF₆[−] ion. Fluoride abstraction from PF₆[−] has

* To whom correspondence should be addressed. Tel: +351-218419172. Fax: +351-218464457. E-mail: ana.martins@ist.utl.pt.

[†] Instituto Superior Técnico.

[‡] University of Nottingham.

(1) Ferreira, M. J.; Martins, A. M. *Coord. Chem. Rev.* **2006**, *250*, 118–132.

(2) McMeeking, J.; Gao, X.; Spence, R. E. V. H.; Brown, S. J.; Jeremic, D. Patent WO 99/14250, 1999.

(3) Dias, A. R.; Duarte, M. T.; Fernandes, A. C.; Fernandes, S.; Marques, M. M.; Martins, A. M.; da Silva, J. F.; Rodrigues, S. S. *J. Organomet. Chem.* **2004**, *689*, 203–213.

(4) Nomura, K.; Fujita, K.; Fujiki, M. *J. Mol. Catal. A: Chem.* **2004**, *220*, 133–144.

(5) Nomura, K.; Fujita, K.; Fujiki, M. *Catal. Commun.* **2004**, *5*, 413–417.

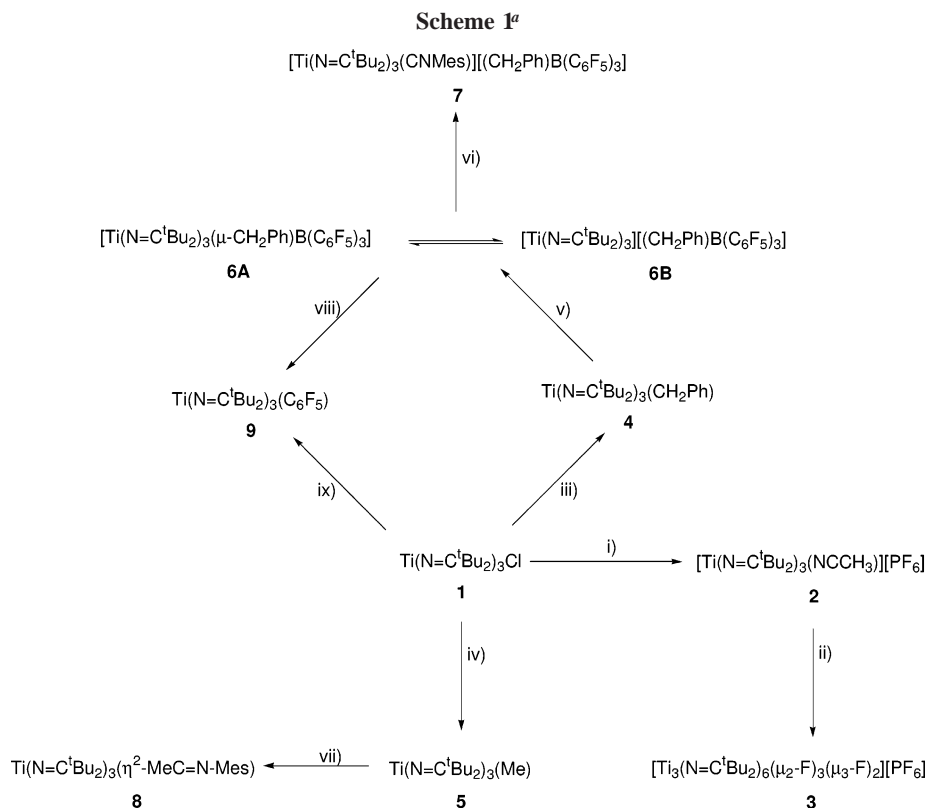
(6) Zhang, H.; Nomura, K. *J. Am. Chem. Soc.* **2005**, *127*, 9364–9365.

(7) Zhang, H.; Nomura, K. *Macromolecules* **2006**, *39*, 5266–5274.

(8) Zhang, S.; Piers, W. E.; Gao, X.; Parvez, M. *J. Am. Chem. Soc.* **2000**, *122*, 5499–5509.

(9) Zhang, S.; Piers, W. E. *Organometallics* **2001**, *20*, 2088–2092.

(10) Martins, A. M.; Marques, M. M.; Ascenso, J. R.; Dias, A. R.; Duarte, M. T.; Fernandes, A. C.; Fernandes, S.; Ferreira, M. J.; Matos, I.; Oliveira, M. C.; Rodrigues, S. S.; Wilson, C. *J. Organomet. Chem.* **2005**, *690*, 874–884.



^a Legend: (i) TlPF₆, CH₃CN; (ii) CH₂Cl₂/hexane, -20 °C; (iii) CH₂PhMgCl; (iv) LiMe; (v) B(C₆F₅)₃; (vi) C≡NMes; (vii) C≡NMes; (viii) heating above 60 °C; (ix) C₆F₅MgCl.

very rarely been reported¹¹ and reflects the extremely acidic nature and accessibility of the cationic metal center. The removal of one ketimide ligand from the metal coordination sphere is most probably promoted by the solvent that should act as a proton source. The proton and carbon NMR spectra of **3** show only one set of signals for the ketimide ligands. The ¹⁹F NMR spectrum displays one doublet for the PF₆⁻ ion (¹J_{PF} = 705.8 Hz) at -71.0 ppm, one triplet at -63.1 ppm (²J_{FF} = 91.1 Hz) assigned to μ₂-F, and one quartet at -91.2 ppm (²J_{FF} = 91.1 Hz) corresponding to the μ₃-F ligands. According to the literature, the resonances due to μ₂-bridging fluorides appear at lower field than those of μ₃-F ligands, as observed in **3**. In comparison to literature reported values (μ₂-¹⁹F, δ -3.4 to -52.8;¹²⁻¹⁶ μ₃-¹⁹F, δ -10.4 to -130.2^{13,15,17,18}), the μ₂-¹⁹F resonances in **3** are shifted to high field. This shift is notable when it is compared to the value observed for [Ti(μ-NMe₂)-(NMe₂)(μ-F)F]₆ (δ -3.4 ppm). We tentatively suggest that the difference reflects the polar nature of the Ti...F...Ti bond between the hard Lewis acidic metal center and the hard fluoride donor in the cationic [(^tBu₂C=N)₂Ti(μ₂-F)]₃(μ₃-F)₂⁺ core.

The formulation of **3** was confirmed by single-crystal X-ray analysis. The molecular structure of **3** is depicted in Figure 1, and selected bond lengths and angles are given in Table 1.

Compound **3** crystallizes in the monoclinic system, space group *P*2₁/*c* with *a* = 12.479(5) Å, *b* = 13.679(5) Å, *c* = 39.391(5) Å, and β = 92.646(5)°. In the [(^tBu₂C=N)₂Ti(μ₂-F)]₃(μ₃-F)₂⁺ core the three titanium atoms define an equilateral triangle with inner angles between 59.82(8) and 60.20(8)° and Ti-Ti distances between 3.095(3) and 3.107(4) Å. This arrangement is maintained by the five bridging fluoride ligands. The μ₂-fluoride ligands F1, F2, and F3 are coplanar with the titanium atoms and bridge two adjacent metal centers, whereas F4 and F5 are positioned above and below the plane defined by the titanium centers (at 1.1937(62) and 1.2000(61) Å from the plane, respectively), with a μ₃-bridging arrangement between the metals (Figure 1b). The occurrence of Ti-Ti interactions in **3** may be excluded, since the Ti-Ti distances exceed the double of the titanium covalent radius (1.32 Å) by a considerable amount. The Ti-F distances observed in **3** are consistent with values reported in the literature for similar bridging fluorides.^{16,17}

The geometry around each Ti(IV) atom can be considered distorted octahedral. For Ti1 the axial positions are defined by F4 and N2 (N2-Ti1-F4 is the larger angle (172.3(4)°)), while the equatorial positions are occupied by F1, F3, F5, and N1. For Ti2, the axial positions are occupied by N4 and F4 (the N4-Ti2-F4 angle is 165.8(4)°) whereas F1, F2, F5, and N3 define the equatorial positions. The axial positions of Ti3 are occupied by F5 and N5 (the N5-Ti3-F5 angle is 165.2(4)°), while F2, F3, F4, and N6 define the equatorial positions. The ketimide ligands in **3** are positioned above and below the plane defined by the three titanium atoms to minimize steric repulsion (see Figure 1b) and are as usual close to linearity (the Ti-N-C angles lie between 169.4(10) and 177.6(11)°). All other

(11) Jordan, R. F.; Dasher, W. E.; Echols, S. F. *J. Am. Chem. Soc.* **1986**, *108*, 1718-1719.

(12) Shah, S. A. A.; Dorn, H.; Gindl, J.; Noltemeyer, M.; Schmidt, H.-G.; Roesky, H. W. *J. Organomet. Chem.* **1998**, *550*, 1-6.

(13) Demsar, A.; Pevec, A.; Golic, L.; Petricek, S.; Petric, A.; Roesky, H. W. *Chem. Commun.* **1998**, 1029-1030.

(14) Santamaría, C.; Beckhaus, R.; Haase, D.; Saak, W.; Koch, R. *Chem. Eur. J.* **2001**, *7*, 622-626.

(15) Pevec, A.; Demsar, A.; Gramlich, V.; Petricek, S.; Roesky, H. W. *J. Chem. Soc., Dalton Trans.* **1997**, 2215-2216.

(16) Perdih, F.; Pevec, A.; Demsar, A. *J. Fluorine Chem.* **2005**, *126*, 1065-1071.

(17) Schormann, M.; Varkey, S. P.; Roesky, H. W.; Noltemeyer, M. *J. Organomet. Chem.* **2001**, *621*, 310-316.

(18) Perdih, F.; Demsar, A.; Pevec, A.; Petricek, S.; Leban, I.; Giester, G.; Sieler, J.; Roesky, H. W. *Polyhedron* **2001**, *20*, 1967-1971.

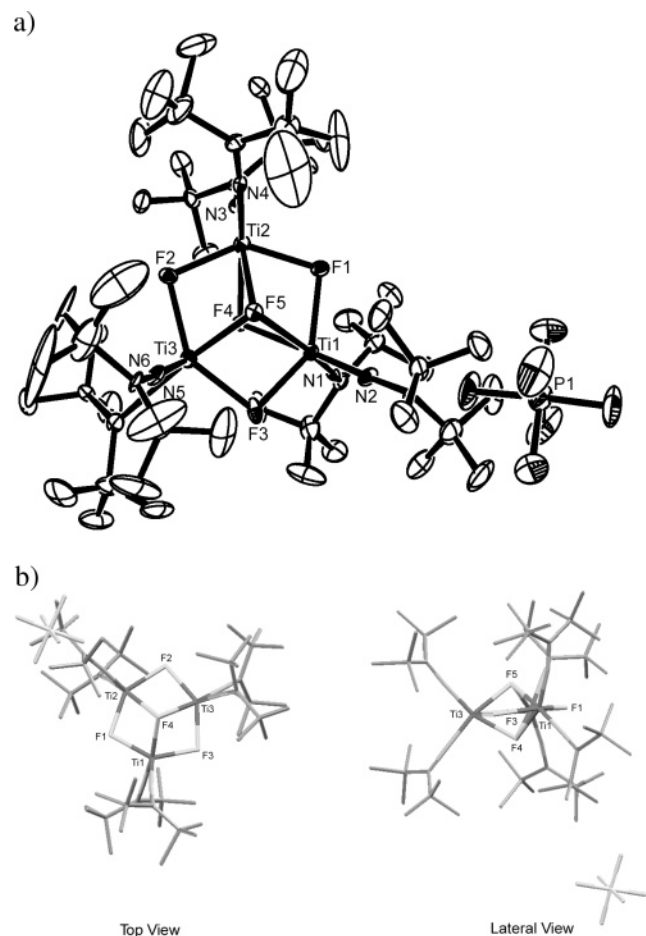


Figure 1. (a) Molecular structure of **3** showing the atom-labeling scheme. Hydrogen atoms are omitted for clarity (thermal ellipsoids are given at the 30% probability level). (b) Molecular structure of **3** showing top and lateral views. Hydrogen atoms are omitted for clarity.

ketimide structural features are similar to those found in the structure of **1**.¹⁰

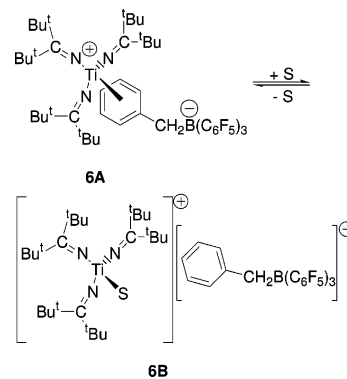
A different approach in the synthesis of cationic tris(ketimide) complexes consisted in the reaction of alkyl derivatives with Lewis acids. Alkyl derivatives were obtained by treatment of $\text{Ti}(\text{N}=\text{C}^t\text{Bu}_2)_3\text{Cl}^{10}$ (**1**) with an excess of PhCH_2MgCl and with an equimolar amount of LiMe to afford $\text{Ti}(\text{N}=\text{C}^t\text{Bu}_2)_3(\text{CH}_2\text{-Ph})$ (**4**) and $\text{Ti}(\text{N}=\text{C}^t\text{Bu}_2)_3(\text{Me})$ (**5**) as a red oil and a bright orange solid, respectively (Scheme 1). In the ^1H and ^{13}C NMR spectra of **4** and **5** the *tert*-butyl resonances are comparable to those found in **1**, whereas the ^{13}C $\text{N}=\text{C}$ signals appear slightly shielded (194.7 ppm for **4** and 194.5 ppm for **5** vs 197.3 ppm for **1**), consistent with somewhat less acidic metal centers. The extreme sensitivity of these compounds to air and moisture led to poor elemental analysis results. Compound formulations were based on the NMR data (see the Supporting Information, Figures S7–S10) and were confirmed by high-resolution mass spectrometry that showed a signal at 559.437 43, corresponding to $[\text{C}_{34}\text{H}_{61}\text{N}_3^{48}\text{Ti}]^-$, for **4**, and a signal at 483.378 85, corresponding to $[\text{C}_{28}\text{H}_{57}\text{N}_3^{48}\text{Ti}]^-$, for **5**, with the correct isotopic patterns.

$\text{Ti}(\text{N}=\text{C}^t\text{Bu}_2)_3(\text{CH}_2\text{Ph})$ (**4**) reacts with $\text{B}(\text{C}_6\text{F}_5)_3$ at -80°C in toluene- d_8 to afford the complex $[\text{Ti}(\text{N}=\text{C}^t\text{Bu}_2)_3(\text{CH}_2\text{Ph})\text{B}(\text{C}_6\text{F}_5)_3]$ (**6**) as a dark red solid in quantitative yield, as determined by NMR. Complex **6** is stable enough to be isolated when the reaction is carried out in a Schlenk tube. However, the extreme sensitivity of **6** to air and moisture led to slightly low experimental values for elemental analysis. In the mass spec-

Table 1. Selected Bond Angles (deg) and Distances (Å) for **3**

Ti1–Ti2	3.107(4)	Ti2–N4	1.837(14)
Ti1–Ti3	3.100(4)	Ti3–F2	2.055(7)
Ti2–Ti3	3.095(3)	Ti3–F3	2.054(8)
Ti1–F1	2.017(7)	Ti3–F4	2.162(7)
Ti1–F3	2.031(7)	Ti3–F5	2.133(7)
Ti1–F4	2.143(7)	Ti3–N5	1.797(13)
Ti1–F5	2.188(7)	Ti3–N6	1.811(14)
Ti1–N1	1.848(14)	N1–C10	1.263(16)
Ti1–N2	1.820(14)	N2–C20	1.261(16)
Ti2–F1	2.043(7)	N3–C30	1.259(16)
Ti2–F2	2.008(7)	N4–C40	1.274(16)
Ti2–F4	2.150(7)	N5–C50	1.250(17)
Ti2–F5	2.043(7)	N6–C60	1.241(16)
Ti2–N3	1.832(14)		
N2–Ti1–F4	172.3(4)	Ti1–F1–Ti2	99.9(3)
N2–Ti1–F5	105.8(4)	Ti2–F2–Ti3	99.2(3)
F3–Ti1–F4	75.1(3)	Ti3–F3–Ti1	98.7(3)
F1–Ti1–F4	75.3(3)	Ti1–F4–Ti2	92.7(3)
F1–Ti1–N2	105.7(4)	Ti1–F4–Ti3	92.1(3)
N1–Ti1–N2	100.2(5)	Ti2–F4–Ti3	91.7(3)
N3–Ti2–F5	162.1(4)	Ti1–F5–Ti2	91.6(3)
N4–Ti2–F4	165.8(4)	Ti1–F5–Ti3	91.7(3)
F1–Ti2–F4	74.6(3)	Ti2–F5–Ti3	92.7(3)
F1–Ti2–N4	106.6(4)	Ti2–Ti1–Ti3	59.82(8)
F4–Ti2–F2	73.6(3)	Ti1–Ti2–Ti3	59.98(8)
F2–Ti2–N4	98.9(4)	Ti1–Ti3–Ti2	60.20(8)
N5–Ti3–F5	165.2(4)	Ti1–N1–C10	169.4(10)
N6–Ti3–F4	161.8(4)	Ti1–N2–C20	177.1(11)
F3–Ti3–F4	74.3(3)	Ti2–N3–C30	175.9(11)
F4–Ti3–F2	72.4(3)	Ti2–N4–C40	176.0(10)
F2–Ti3–N6	100.2(4)	Ti3–N5–C50	177.6(11)
F3–Ti3–N6	104.9(4)	Ti3–N6–C60	172.8(11)

Scheme 2



trum only the anion was detected (603.040 67 for $[\text{C}_{25}\text{H}_7\text{BF}_5]^-$). Nevertheless, NMR data support the formulation of **6** and show that in solution it exists as a mixture of two species that undergo an exchange process (Scheme 2).

Benzyl abstraction is attested by the ^{11}B spectrum, which exhibits a single sharp resonance at -7.5 ppm. In the ^1H , ^{13}C , and ^{19}F NMR spectra two sets of signals, corresponding to species **6A** and **6B**, are observed. The presence of the zwitterionic complex is supported by the value of $\Delta\delta = 4$ ppm ($\Delta\delta = \delta(\text{F}_p) - \delta(\text{F}_m)$) in the ^{19}F spectrum¹⁹ and by the upfield shift of H_p and H_m benzyl resonances (δ 6.12 and 6.33 ppm) in comparison to those of $[\text{PhCH}_2\text{B}(\text{C}_6\text{F}_5)_3]^-$.²⁰ The ^{19}F resonances due to **6B** are consistent with a cationic species ($\Delta\delta = 2.5$ ppm for the free anion). In the ^1H NMR spectrum the H_p and H_m resonances overlap at 7.01 ppm.^{19–25} Two sets of *tert*-butyl (δ 1.05 (**6B**) and 1.00 ppm (**6A**)) and CH_2Ph resonances (δ 3.46

(19) Horton, A. D.; de With, J. *Chem. Commun.* **1996**, 1375–1376.

(20) Pellecchia, C.; Grassi, A.; Zambelli, A. *J. Mol. Catal.* **1993**, *82*, 57–65.

(21) Pellecchia, C.; Immirzi, A.; Grassi, A.; Zambelli, A. *Organometallics* **1993**, *12*, 4473–4478.

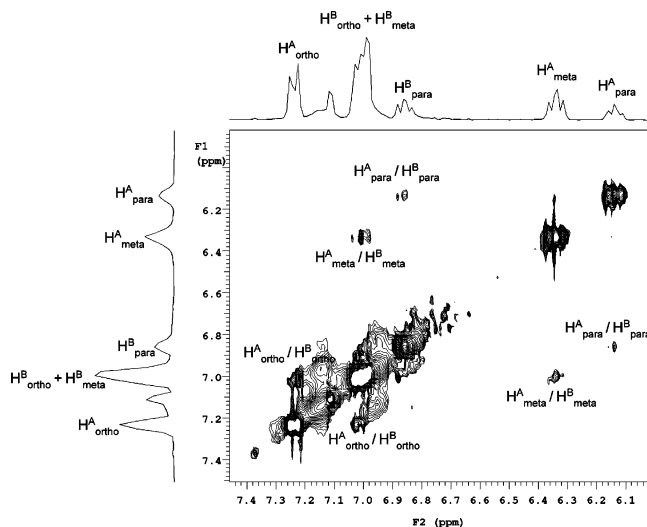


Figure 2. NOESY of **6** showing the dynamic exchange between the two phenyl rings.

(**6A**) and 3.40 ppm (**6B**) are observed in the ^1H spectrum, and the ^{13}C NMR data also reveal two sets of *tert*-butyl signals (δ 30.4 and 46.8 ppm for **6A** and 30.6 and 44.8 ppm for **6B**). The resonances due to the methylenic benzyl carbons are not visible. They may either be broadened by ^{11}B coupling or overlapped by the methyl resonances of the *tert*-butyl groups. **6B** is formulated as a solvent adduct, although solvent coordination is not detected in the NMR spectrum, due to rapid exchange with free solvent. The existence of two species in solution is corroborated by NOESY experiments, which show two different CH_2 groups correlating with two different ortho protons (Figure 2). The same experiment established that the two species exist in dynamic exchange, anion coordination being thus a fluxional process, as represented in Scheme 2.

The $\text{N}=\text{C}$ imine carbon chemical shift for **6B** is shifted downfield in comparison to that for complex **1** (205.6 ppm vs 197.3 ppm, respectively), consistent with a more acidic metal center. However, the same is not applied to **6A**, which exhibits a ^{13}C $\text{N}=\text{C}$ chemical shift of 191.7 ppm. This implies a strong coordination of the anion to the metal center, as supported by the large $\Delta\delta$ value encountered in the ^{19}F spectra^{23,26} and the upfield shift of the meta and para proton resonances in the ^1H spectrum.²⁷

The equilibrium depicted in Scheme 2 is temperature- and solvent-dependent. At low temperatures in toluene- d_8 (<20 °C) it is shifted toward **6B**, whereas at 20 °C and above, **6A** becomes predominant. In bromobenzene- d_5 , **6A** is always the major species and above 50 °C is the only one detected in solution.

The equilibrium between **6A** and **6B** is stopped upon addition of an L-type σ -donor. Treatment of **6** with 1 equiv of $\text{C}\equiv\text{NMe}$ s afforded $[\text{Ti}(\text{N}=\text{C}^t\text{Bu})_3(\text{C}\equiv\text{NMe})][(\text{CH}_2\text{Ph})\text{B}(\text{C}_6\text{F}_5)_3]$ (**7**), which was characterized by NMR. The ^1H NMR spectrum shows the anion aromatic protons between 7.00 and 7.20 ppm, in accordance with the presence of free anion. Consistently, in the ^{19}F NMR spectrum, $\Delta\delta$ is 2.4 ppm in toluene- d_8 and 2.6 ppm

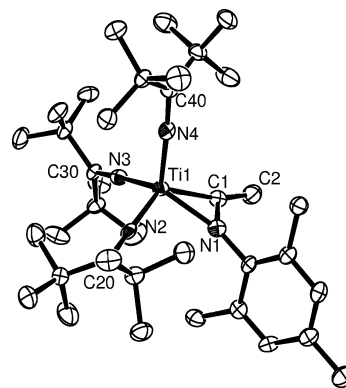


Figure 3. Molecular structure of **8** showing the atom-labeling scheme. Hydrogen atoms are omitted for clarity (thermal ellipsoids are given at the 50% probability level).

Table 2. Selected Bond Angles (deg) and Distances (Å) for **8**

Ti1–C1	2.104(6)	N2–20	1.257(8)
Ti1–N1	2.074(5)	N3–C30	1.259(7)
Ti1–N2	1.916(5)	N4–C40	1.273(7)
Ti1–N3	1.899(5)	C1–C2	1.498(9)
Ti1–N4	1.882(5)	N4–(N1–C1–N2–N3)	2.5087(47)
N1–C1	1.282(7)		
N1–Ti1–C1	35.7(2)	Ti1–C1–C2	163.2(5)
N1–Ti1–N2	95.2(2)	Ti1–N1–C3	158.6(4)
N2–Ti1–N3	101.4(2)	Ti1–N2–C20	173.7(4)
N3–Ti1–C1	102.7(2)	Ti1–N3–C30	175.2(4)
C1–Ti1–N4	106.8(2)	Ti1–N4–C40	175.4(4)
N1–Ti1–N4	116.7(2)	(N1–C1–N2–N3)–(Mes)	77.30(19)
N2–Ti1–N4	109.6(2)	(Mes)–(Ti1–N4)	13.81(36)
N3–Ti1–N4	104.2(2)	(Mes)–(N1–C1)	63.29(44)

in bromobenzene- d_5 . The isonitrile carbon resonance in the ^{13}C NMR spectrum was found at 143.7 ppm, in accordance with values of group 4 coordinated isonitriles reported in the literature.^{28–30} Coordination of the isonitrile was further confirmed by the observation of NOE between the *o*-methyl groups of the mesityl moiety and the ^tBu groups of the ketimide ligands. The imine carbon resonance appears at 202.3 ppm, close to the value observed for **6B** (205.6 ppm).

Further insertions of $\text{C}\equiv\text{NMe}$ s have not been observed at 50 °C for 18 h in the presence of an excess of isonitrile. The lack of isonitrile insertion in the Ti–N bond reflects strong π -bonding between the ketimide ligands and the metal center. A steric hindrance does not play any relevant influence in this result, since insertion of the isocyanide in the Ti–C bond of $\text{Ti}(\text{N}=\text{C}^t\text{Bu})_3(\text{Me})$ (**5**) occurs readily and quantitatively at room temperature, leading to $\text{Ti}(\text{N}=\text{C}^t\text{Bu})_3(\eta^2\text{-MeC}=\text{N-Mes})$ (**8**), which is obtained as a bright red crystalline solid (Scheme 1). Compound formulation was confirmed by high-resolution mass spectrometry that gave a signal at m/z 628.489 12 corresponding to $[\text{C}_{38}\text{H}_{68}\text{N}_4^{48}\text{Ti}]^-$, with the correct isotopic pattern. The inserted methyl group shows significantly different ^1H and ^{13}C resonances in comparison to those found in **5** (2.30 ppm vs 1.10 ppm and 23.0 ppm vs 41.3 ppm, respectively), in agreement with values found in the literature for similar ligands.^{31,32} η^2 -

(22) Horton, A. D.; de With, J.; van der Linden, A.; van der Weg, H. *Organometallics* **1996**, *15*, 2672–2674.

(23) Horton, A. D.; de With, J. *Organometallics* **1997**, *16*, 5424–5436.

(24) Shafir, A.; Arnold, J. *Organometallics* **2003**, *22*, 567–575.

(25) Pellecchia, C.; Grassi, A.; Immirzi, A. *J. Am. Chem. Soc.* **1993**, *115*, 1160–1162.

(26) Pindado, G. J.; Thornton-Pett, M.; Hursthouse, M. B.; Coles, S. J.; Bochmann, M. *J. Chem. Soc., Dalton Trans.* **1999**, 1663–1668.

(27) Amor, F.; Butt, A.; du Plooy, K. E.; Spaniol, T. P.; Okuda, J. *Organometallics* **1998**, *17*, 5836–5849.

(28) Pflug, J.; Bertuleit, A.; Kehr, G.; Fröhlich, R.; Erker, G. *Organometallics* **1999**, *18*, 3818–3826.

(29) Ahlers, W.; Erker, G.; Fröhlich, R. *J. Organomet. Chem.* **1998**, *571*, 83–89.

(30) Ahlers, W.; Erker, G.; Fröhlich, R. *Eur. J. Inorg. Chem.* **1998**, 889–895.

(31) Martins, A. M.; Ascenso, J. R.; Azevedo, C. G.; Dias, A. R.; Duarte, M. T.; da Silva, J. F.; Veiros, L. F.; Rodrigues, S. S. *Organometallics* **2003**, *22*, 4218–4228.

(32) Bochmann, M.; Wilson, L. M.; Hursthouse, M. B.; Short, R. L. *Organometallics* **1987**, *6*, 2556–2563.

Iminoacyl coordination was inferred from the ^{13}C chemical shift of the $\text{N}=\text{C}$ carbons of the ketimide ligands, which is significantly shifted to high field in comparison with that of **5** (184.6 vs 194.5 ppm in **5**) and from the ^{13}C resonance of the $\text{Mes}-\text{N}=\text{C}$ iminoacyl carbon (256.2 ppm), which is close to those reported in the literature for similar ligands.^{31,32}

These results are consistent with the molecular structure of **8** that is depicted in Figure 3. Selected bond lengths and angles are given in Table 2. The compound crystallizes in the triclinic system, space group $P2_1/n$. The geometry around the titanium is best described as distorted square pyramidal, with the base defined by C1, N1, N2, and N3 (the maximum deviation from the plane is 0.1354(56) Å for C1) and the tip of the pyramid occupied by N4. The titanium lies at 0.6398(10) Å above the basal plane. The iminoacyl ligand is η^2 -coordinated to the metal, since N1 and C1 lie at similar distances from the titanium center (2.074(5) and 2.104(6) Å, respectively) and the N1–C1 distance is comparable to those of other titanium η^2 -iminoacyl complexes found in the literature.^{33,34} The methyl and mesityl groups pull away from the N1–C1 bond to minimize steric repulsion (with angles of 163.2 and 158.6(4)°, respectively). The mesityl group makes an angle of 63.29(44)° with the N1–C1 bond and of 77.30(19)° with the plane that defines the base of the square pyramid and is almost aligned with the Ti–N4 axis (13.81–(36)°). This orientation is adopted to minimize steric effects, since there are no π -contacts between the mesityl groups of adjacent molecules in the unit cell. The ketimide ligands are linear (angles between 173.7(4)° and 175.4(4)°) with Ti–N distances commonly found in group 4 ketimide complexes.¹⁰ The Ti–N2 distance is slightly larger than the other two, possibly due to the trans effect of the iminoacyl ligand.

The compound $[\text{Ti}(\text{N}=\text{C}^i\text{Bu}_2)_3][(\text{CH}_2\text{Ph})\text{B}(\text{C}_6\text{F}_5)_3]$ (**6**) is stable in toluene and bromobenzene solutions up to 60 °C. Above this temperature, however, partial decomposition is observed with formation of $\text{Ti}(\text{N}=\text{C}^i\text{Bu}_2)_3(\text{C}_6\text{F}_5)$ (**9**), obtained by C_6F_5 transfer from the anion to the titanium center. This relatively common rearrangement^{8,35,36} is not the only process occurring in solution, since other minor species, which have not been identified, were detected. Nevertheless, **9** is clearly the major component in solution, which makes C_6F_5 transfer the preferred thermal decomposition pathway for **6**. Formation of **9** was initially inferred by the ^{19}F NMR spectrum, which showed a new set of signals in which the F_o resonance appears at –112.2 ppm (vs –123.0 ppm for F_o of **6**) and resonances attributed to $(\text{CH}_2\text{Ph})\text{B}(\text{C}_6\text{F}_5)_2$ at –129.6 ppm (F_o), –155.6 ppm (F_p), and –161.0 ppm (F_m).⁸ This assignment was made possible by ^{19}F COSY NMR. Furthermore, the formulation of **9** was confirmed by direct synthesis via alkylation of **1** with $\text{C}_6\text{F}_5\text{-MgCl}$ (Scheme 1) that led to quantitatively to $\text{Ti}(\text{N}=\text{C}^i\text{Bu}_2)_3(\text{C}_6\text{F}_5)$ (**9**) as a bright red solid. The ^{13}C $\text{N}=\text{C}$ chemical shift of **9**, which appears shifted downfield in comparison with that of **1**, is consistent with the presence of a more electron withdrawing group (199.5 ppm for **9** vs 197.3 ppm for **1**). The ^{19}F NMR spectrum of the compound shows that it is involved in an intramolecular fluxional process, as depicted in Figure 4, which shows the temperature variation study of the ^{19}F spectra and the ^{19}F NMR spectrum at –40 °C. Between –80 and 110 °C **9**

exists in toluene- d_8 as a mixture of two species that are in equilibrium and displays signals with complex multiplicity.

Two F_o resonances at –111.6 and –136.8 ppm are assigned to **9A** and **9B**, respectively (Scheme 3). The $\text{Ti}\cdots\text{F}$ interaction in **9B** is responsible for the shift of the F_o resonance to high field^{8,35} and for the observation of five different resonances for the C_6F_5 ring.^{37–40} However, the similarity between the chemical shifts of the two F_o and the two F_m resonances is indicative of a fast exchange between the coordinated and free F_o substituents (species **9B** in Chart 2). Accordingly, the five fluorine nuclei in complex **9B** give rise to three complex peaks that are integrated in the ratio 2:1:2 and correspond to F_o , F_p , and F_m , respectively. At 110 °C, **9B** is fully converted to the solvent adduct $\text{Ti}(\text{N}=\text{C}^i\text{Bu}_2)_3(\text{C}_6\text{F}_5)(\text{solv})$ (**9A**), which is responsible for the other set of fluorine resonances observed in the ^{19}F NMR spectra. The F_o resonance at –111.6 ppm is indicative of no interaction between the ortho fluorides and the titanium center.^{8,35} Once again, the multiplicity of the set of signals attributed to **9A** indicates that there are five different fluorine atoms in the ring which appear as three average complex signals. This effect might result from hindered rotation around the Ti– C_6F_5 bond. The fact that the multiplicity of fluorine resonances is temperature-independent suggests that the coordination of the solvent is ultimately responsible for the restriction of C_6F_5 rotation. This idea is reinforced by the observation that a change in the solvent dramatically changes the **9A**:**9B** ratio. Spectra run at room temperature in toluene- d_8 show both species whereas in C_6D_6 the spectrum at the same temperature shows only **9A**, a result that is observed in toluene- d_8 at 110 °C.

The equilibrium constant ($K = C_{9A}/C_{9B}$) was calculated from the ^{19}F NMR integral ratio in the temperature range of 169–364 K. The plot of $\ln K$ versus $1/T$ (Figure S24 and Tables S1–S3 in Supporting Information) led to the values of $\Delta H = 2.38 \pm 0.4 \text{ kJ mol}^{-1}$ and $\Delta S = 18 \pm 2 \text{ J mol}^{-1} \text{ K}^{-1}$. These very small values attest to the fact that the process occurs with negligible energy variation, which is consistent with the proposed equilibrium that does not involve variation in the metal coordination number or major rearrangements in the coordination sphere.

Concluding Remarks

The results discussed above indicate that it is possible to stabilize species of the type $[\text{Ti}(\text{N}=\text{C}^i\text{Bu}_2)_3]^+$, provided that the correct counterion is present. Counterions that establish π interactions with the cation, such as $[(\text{PhCH}_2)\text{B}(\text{C}_6\text{F}_5)_3]^-$, lead to more stable compounds than counterions that establish σ interactions, such as PF_6^- . For the latter, the acidity of the metal center is strong enough to abstract fluorine from the anion, as attested to by the formation of $[\text{Ti}_3(\text{N}=\text{C}^i\text{Bu}_2)_6(\mu_2\text{-F})_3(\mu_3\text{-F})_2]\text{-}[\text{PF}_6]$ (**3**). This result, together with the fluxional processes observed in solution for $[\text{Ti}(\text{N}=\text{C}^i\text{Bu}_2)_3][(\text{PhCH}_2)\text{B}(\text{C}_6\text{F}_5)_3]$ (**6**) and $\text{Ti}(\text{N}=\text{C}^i\text{Bu}_2)_3(\text{C}_6\text{F}_5)$ (**9**), show that titanium ketimide complexes are hard Lewis acids. In addition, ketimide ligands

(33) Chamberlain, L. R.; Durfee, L. D.; Fanwick, P. E.; Kobriger, L.; Latesky, S. L.; McMullen, A. K.; Rothwell, I. P.; Folting, K.; Huffman, J. C.; Streib, W. E.; Wang, R. *J. Am. Chem. Soc.* **1987**, *109*, 390–402.

(34) van Bolhuis, F.; de Boer, E. J. M.; Teuben, J. H. *J. Organomet. Chem.* **1979**, *170*, 299–308.

(35) Gómez, R.; Gómez-Sal, P.; del Real, P. A.; Royo, P. *J. Organomet. Chem.* **1999**, *588*, 22–27.

(36) Guérin, F.; Stewart, J. C.; Beddie, C.; Stephan, D. W. *Organometallics* **2000**, *19*, 2994–3000.

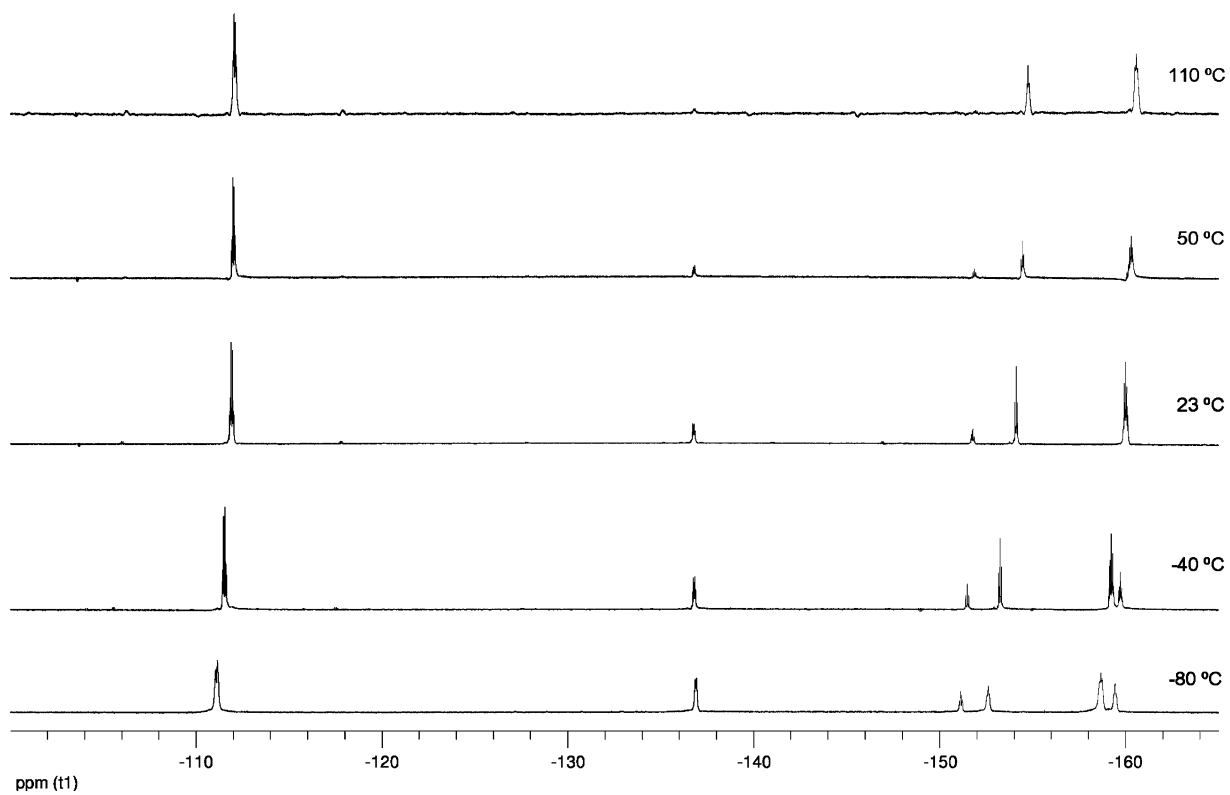
(37) Jia, L.; Yang, X.; Stern, C. L.; Marks, T. J. *Organometallics* **1997**, *16*, 842–857.

(38) Burlakov, V. V.; Arndt, P.; Baumann, W.; Spannenberg, A.; Rosenthal, U.; Letov, A. V.; Lyssenko, K. A.; Korlyukov, A. A.; Strunkina, L. I.; Minacheva, M. K.; Shur, V. B. *Organometallics* **2001**, *20*, 4072–4079.

(39) Woodman, T. J.; Thornton-Pett, M.; Hughes, D. L.; Bochmann, M. *Organometallics* **2001**, *20*, 4080–4091.

(40) Siedle, A. R.; Newmark, R. A.; Lammana, W. M.; Huffman, J. C. *Organometallics* **1993**, *12*, 1491–1492.

a)



b)

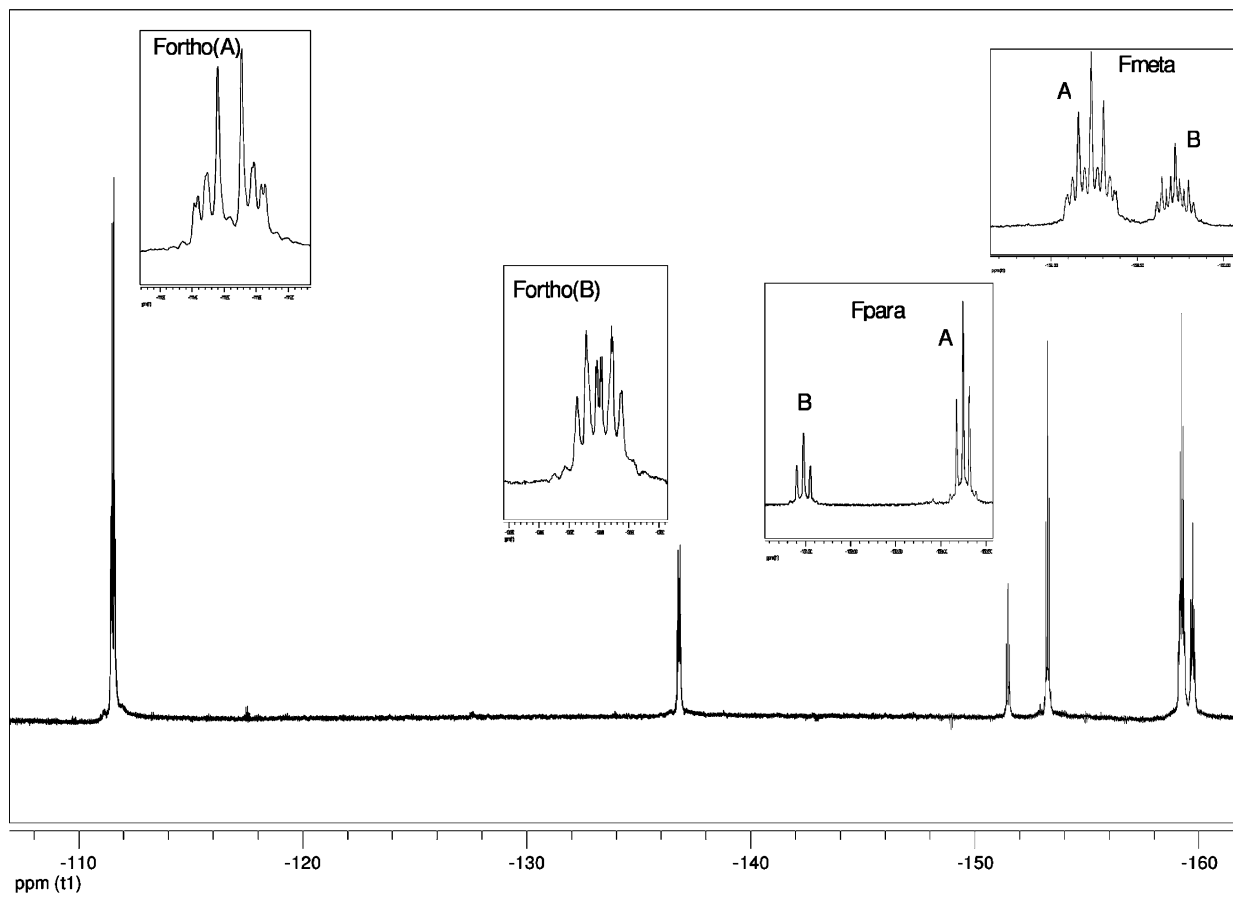
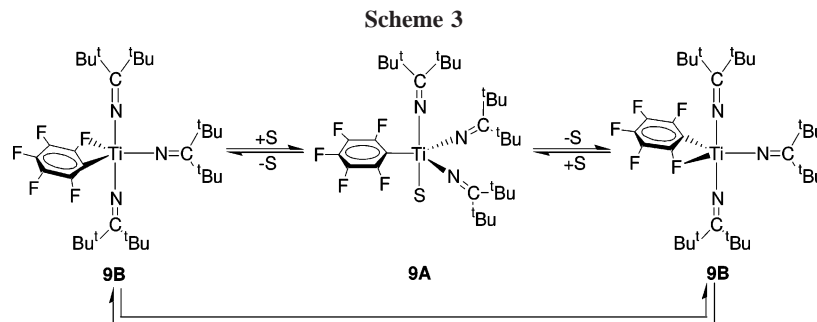


Figure 4. (a) Temperature study of ^{19}F NMR spectra of **9** in toluene- d_8 . (b) ^{19}F NMR spectrum of **9** at $-40\text{ }^\circ\text{C}$ in toluene- d_8 .



fail to offer good steric protection to the metal center, allowing the formation of small aggregates as well as metal–solvent interactions.

Experimental Section

All manipulations were carried out under nitrogen, using either standard Schlenk-line or drybox techniques.

Solvents were predried using 4 Å molecular sieves, refluxed over sodium–benzophenone (diethyl ether, tetrahydrofuran, and toluene) or calcium hydride (dichloromethane, acetonitrile, and *n*-hexane) under an atmosphere of nitrogen, and collected by distillation. Deuterated solvents were dried with molecular sieves and freeze–pump–thaw–degassed prior to use.

^1H , ^{13}C , ^{19}F , ^{31}P , and ^{11}B NMR spectra were recorded on a Varian Unity 300 instrument, at 298 K unless stated otherwise. ^1H and ^{13}C NMR spectra were referenced internally to residual protio-solvent (^1H) or solvent (^{13}C) resonances and reported relative to tetramethylsilane (δ 0). ^{19}F , ^{31}P , and ^{11}B spectra were referenced externally to CF_3COOH (δ -76 ppm), H_3PO_4 , and $\text{BF}_3\cdot\text{Et}_2\text{O}$, respectively. Peak assignments were based on one- and two-dimensional NOE experiments and on $^{13}\text{C}\{^1\text{H}\}$ – ^1H hetero-correlations, as appropriate.

High-resolution electron ionization (EI) mass spectra were obtained by a Fourier transform ion cyclotron resonance mass spectrometer (Finnegan FT/MS 2001-DT spectrometer), equipped with a 3 T superconducting magnet. Elemental analyses were obtained from the Laboratório de Análises do IST (Fisons Instrument 1108).

PhCH_2MgCl (1.5 mol dm^{-3} in ether) and $\text{C}_6\text{F}_5\text{MgCl}$ (0.5 mol dm^{-3} in ether) were purchased from Aldrich and titrated by the usual methods before use. LiMe (1.8 M in ether) was purchased from Merck and titrated prior to use. The compounds $\text{LiN}=\text{C}^t\text{Bu}_2$,⁴¹ $\text{Ti}(\text{N}=\text{C}^t\text{Bu}_2)_3\text{Cl}$ (**1**),¹⁰ $\text{B}(\text{C}_6\text{F}_5)_3$,⁴² $\text{C}\equiv\text{NMe}$,⁴³ and TIPF_6 ⁴⁴ were prepared according to literature methods.

[Ti(N=C^tBu)₃(N≡CCH₃)](PF₆) (2). A solution of **1** (0.512 g, 1.02 mmol) in acetonitrile was added to a suspension of TIPF_6 (0.394 g, 1.13 mmol) in acetonitrile, cooled to -30 °C. A bright orange solution formed immediately. The mixture was warmed to room temperature and was stirred overnight. The mixture was filtered through Celite, but a solid residue persisted. Solvent removal afforded a bright yellow solid (0.607 g, 91% yield) that upon standing at room temperature turns green. ^1H NMR (CD_3CN , 300 MHz): δ 1.26 (s, 54H, ^tBu). ^{19}F NMR (CD_3CN , 282 MHz): δ -67.4 (d, $^1J_{\text{F-P}} = 705.8$ Hz). ^{31}P NMR (CD_3CN , 121 MHz): δ -138.7 (ps t, $J = 708.6$ Hz). $^{13}\text{C}\{^1\text{H}\}$ NMR (CD_3CN , 75 MHz): δ 201.6 (C=N), 43.1 ($\text{C}(\text{CH}_3)_3$), 29.7 ($\text{C}(\text{CH}_3)_3$), 2.03 (NCCCH₃). ^1H NMR (CD_2Cl_2 , 300 MHz): δ 1.98 (br s, CH_3CN), 1.19 (s, 13.7

H, ^tBu). ^{19}F NMR (CD_2Cl_2 , 282 MHz): δ -70.87 (d, $^1J_{\text{F-P}} = 708.9$ Hz). ^{31}P NMR (CD_2Cl_2 , 121 MHz): δ -141.9 (ps t, $^1J_{\text{F-P}} = 708.6$ Hz). $^{13}\text{C}\{^1\text{H}\}$ NMR (CD_2Cl_2 , 75 MHz): δ 201.5 (C=N), 42.4 ($\text{C}(\text{CH}_3)_3$), 29.9 ($\text{C}(\text{CH}_3)_3$), 2.03 (NCCCH₃).

[Ti₃(N=C^tBu)₆(μ_2 -F)₃(μ_3 -F)₂](PF₆) (3). Compound **2** was dissolved in CH_2Cl_2 and hexane was added as a double layer. Solvent diffusion was allowed to proceed slowly at -20 °C, affording dark green needles. ^1H NMR (CD_2Cl_2 , 300 MHz): δ 1.38 (s, 108 H, ^tBu). ^{19}F NMR (CD_2Cl_2 , 282 MHz): δ -63.1 (t, $^2J_{\text{FF}} = 91.1$ Hz, μ_2 -F), -71.0 (d, $^1J_{\text{F-P}} = 705.8$ Hz, PF_6^-), -91.2 (q, $^2J_{\text{FF}} = 91.1$ Hz, μ_3 -F). ^{31}P NMR (CD_2Cl_2 , 121 MHz): δ -141.9 (ps t, $^1J_{\text{F-P}} = 711.5$ Hz). $^{13}\text{C}\{^1\text{H}\}$ NMR (CD_2Cl_2 , 75 MHz): δ 42.6 ($\text{C}(\text{CH}_3)_3$), 29.6 ($\text{C}(\text{CH}_3)_3$). Anal. Calcd for $\text{C}_{54}\text{H}_{108}\text{F}_{11}\text{N}_6\text{P}_6\text{Ti}_3$: C, 52.94; H, 8.89; N, 6.86. Found: C, 44.40; H, 8.49; N, 5.49. The elemental analysis results of the crystals were repeated, and the results always showed deviations from the calculated values. The NMR spectra (see Figures S3–S6 in the Supporting Information) and the analysis of several crystals always confirmed the results. The discrepancy is probably due to the high fluorine content of the sample.

Ti(N=C^tBu)₃(CH₂Ph) (4). A solution of **1** (0.835 g, 1.66 mmol) in 40 mL of hexane was cooled to -50 °C, and a solution of $\text{PhCH}_2\text{-MgCl}$ in ether (1.5 M, 4.18 mmol) was added. A white precipitate formed immediately. The mixture was warmed slowly to room temperature over a period of 2.5 h. The solvent was pumped off and the residue extracted with hexane. Solvent removal afforded 0.890 g of a red oil (96.0% yield). ^1H NMR (C_7D_8 , 300 MHz): δ 7.13 (m, 2H, H_o), 7.11 (m, 2H, H_m), 6.81 (t, $J = 6.9$ Hz, 1H, H_p), 2.89 (s, 2H, CH_2), 1.21 (s, 54H, ^tBu). $^{13}\text{C}\{^1\text{H}\}$ NMR (C_7D_8 , 75 MHz): δ 194.7 (C=N), 149.1 (C_{ipso}), 128.1 (C_o), 127.4 (C_m), 121.0 (C_p), 68.8 (CH_2), 45.6 ($\text{C}(\text{CH}_3)_3$), 30.9 ($\text{C}(\text{CH}_3)_3$). EI/FT ICR-MS: 559.437 43 (100) ($[\text{C}_{34}\text{H}_{61}\text{N}_3^{48}\text{Ti}]^+$). Anal. Calcd for $\text{C}_{34}\text{H}_{61}\text{N}_3\text{Ti}$: C, 72.96; H, 10.98; N, 7.51. Found: C, 70.04; H, 11.47; N, 6.82.

Ti(N=C^tBu)₃(Me) (5). LiMe (1.8 M, 0.88 mmol) was added to a solution of **1** (0.441 g, 0.88 mmol) in 20 mL of hexane cooled to -50 °C. The reaction medium turned bright orange immediately. The mixture was warmed to room temperature, and the solvent was pumped off. Subsequent extraction with hexane afforded 0.369 g of a bright orange solid (87% yield). ^1H NMR (C_7D_8 , 300 MHz): δ 1.30 (s, 54H, ^tBu), 1.10 (s, 3H, Ti–Me). $^{13}\text{C}\{^1\text{H}\}$ NMR (C_7D_8 , 75 MHz): δ 194.5 (C=N), 45.5 ($\text{C}(\text{CH}_3)_3$), 41.3 (Ti–CH₃), 31.0 ($\text{C}(\text{CH}_3)_3$). EI/FT ICR-MS: 483.378 85 (100) ($[\text{C}_{28}\text{H}_{57}\text{N}_3^{48}\text{Ti}]^+$). Anal. Calcd for $\text{C}_{28}\text{H}_{57}\text{N}_3\text{Ti}$: C, 69.53; H, 11.87; N, 8.69. Found: C, 67.86; H, 12.18; N, 8.41.

[Ti(N=C^tBu)₃][(CH₂Ph)B(C₆F₅)₃] (6). **Method A.** Complex **4** (0.122 g, 0.22 mmol) was dissolved in 0.3 mL of toluene-*d*₈ in a NMR tube adapted to be sealed. The solution was degassed and frozen, and $\text{B}(\text{C}_6\text{F}_5)_3$ (0.122 g, 0.24 mmol) in 0.3 mL of toluene-*d*₈ was added. The tube was sealed under vacuum and was unfrozen in a bath at -80 °C, prior to its introduction in the NMR instrument, where it was warmed to room temperature, as it was monitored. The reaction was complete instantly at -80 °C, in quantitative yield.

Method B. Complex **4** (0.606 g, 1.08 mmol) was dissolved in approximately 20 mL of toluene, and the solution was cooled to -80 °C. $\text{B}(\text{C}_6\text{F}_5)_3$ (0.607 g, 1.19 mmol) in 30 mL of toluene was added, and a dark red precipitate was readily formed. The reaction

(41) Clegg, W.; Snaith, R.; Shearer, H. M. M.; Wade, K.; Whitehead, G. *J. Chem. Soc., Dalton Trans.* **1983**, 1309–1317.

(42) Chernega, A.; Graham, A. J.; Green, M. L. H.; Haggitt, J. L.; Lloyd, J.; Mehnert, C. P.; Metzler, N.; Souter, J. *J. Chem. Soc., Dalton Trans.* **1997**, 2293–2303.

(43) Obrecht, R.; Hermann, R.; Ugi, I. *Synthesis* **1985**, 04, 400–401.

(44) Herrmann, W. A.; Salzer, A. *Literature, Laboratory Techniques and Common Starting Materials*; Thieme: Stuttgart, Germany, 1996.

mixture was warmed slowly to 10 °C, and the solution was filtered off. The residue was washed with hexane, affording 0.790 g of a dark red solid (68% yield). ¹H NMR (C₇D₈, 10 °C, 300 MHz): δ 7.24 (d, 7.2 Hz, H^A_o), 7.01 (m, H^B_o + H^B_m), 6.85 (m, H^B_p), 6.33 (t, 7.5 Hz, H^A_m), 6.12 (t, 7.5 Hz, H^A_p), 3.46 (s, CH₂B^A), 3.40 (s, CH₂B^B), 1.04 (t, H^{Bu}_A), 0.97 (t, H^{Bu}_B). ¹⁹F NMR (C₇D₈, 10 °C, 282 MHz): δ -123.0 (d, *J* = 22.6 Hz, 2F, F^A_o), -123.6 (d, *J* = 20 Hz, 2F, F^B_o), -154.5 (t, *J* = 20.9 Hz, 1F, F^A_p), -157.7 (t, *J* = 20.9 Hz, 1F, F^B_p), -158.5 (t, *J* = 20.9 Hz, 2F, F^A_m), -160.2 (t, *J* = 20.9 Hz, 2F, F^B_m). ¹¹B NMR (C₇D₈, 10 °C, 96 MHz): δ -7.5. ¹³C{¹H} NMR (C₇D₈, 75 MHz): δ 205.6 (N=C^B), 191.7 (N=C^A), 150.5 and 147.5 (d, *J*_{CF} = 225 Hz, C_o-F), 149.4 (C_{ipso} CH₂Ph^B), 138.9 and 136.3 (d, *J*_{CF} = 195 Hz, C_m-F), 127.2 (C_o), 126.8 (C_m), 123.0 (C_p^A), 122.3 (C_p^B), 46.8 (C(CH₃)₃^A), 44.8 (C(CH₃)₃^B), 31.6 (BCH₂, br), 30.6 (CH₃^B), 30.4 (CH₃^A). ¹H NMR (C₆D₅Br, 300 MHz): δ 7.65–7.10 (br, H_{arom}, 5H), 3.82 (br s, CH₂, 2H), 1.57 and 1.53 (s, t, H_{bu}, 54 H, ~1.5:1). ¹H NMR (C₆D₅Br, 50 °C, 300 MHz): δ 7.57 (d, 7.2 Hz, H_o, 2H), 7.37 (t, H_m, 7.0 Hz, 2H), 7.23 (t, H_p, 6.9 Hz, 1H), 3.80 (s, CH₂, 2H), 1.56 (s, t, H_{bu}, 54 H). ¹⁹F NMR (C₆D₅Br, 282 MHz): δ -128.4 (br, 2F, F_o^{A+B}), -158.9 (t, *J* = 20.3, 1F, F_p^A), -161.8 (br, 1F, F_p^B), -162.8 (br, 2F, F_m^A), -164.5 (br, 2F, F_m^B); **6A:6B** = 1.4:1. ¹⁹F NMR (C₆D₅Br, 50 °C, 282 MHz): δ -128.6 (d, *J* = 20.7 Hz, 2F, F_o), -159.9 (br, 2F, F_p), -163.9 (br, 1F, F_m). ¹¹B NMR (C₆D₅Br, 96 MHz): δ -12.8. ¹³C{¹H} NMR (C₆D₅Br, 75 MHz): δ 211.6 (N=C^B), 205.2 (N=C^A), 148.8 (C_{ipso}), 150.0 and 146.8 (d, *J*_{CF} = 238.6 Hz, C_o-F), 138.9 and 135.9 (d, *J*_{CF} = 226.4 Hz, C_p-F), 138.1 and 134.9 (d, *J*_{CF} = 240.3 Hz, C_m-F), 128.9 (C_o), 127.0 (C_m), 122.7 (C_p), 46.4 (C(CH₃)₃^A), 41.7 (C(CH₃)₃^B), 30.1 (CH₃^{A+B}). EI/FT ICR-MS: 603.040 67 (100) ([C₂₅H₇BF₁₅]⁻). Anal. Calcd for C₅₂H₆₁BF₁₅N₃-Ti: C, 58.28; H, 5.74; N, 3.92. Found: C, 57.02; H, 5.85; N, 3.75.

[Ti(N=C^{Bu})₃(C≡NMe)s][[(CH₂Ph)B(C₆F₅)₃] (7). Compound **6** (0.030 g, 0.03 mmol) was dissolved in 300 μL of toluene-*d*₈, and C≡NMe (0.004 g, 0.03 mmol), also in 300 μL of toluene-*d*₈, was added. A dark red oil formed immediately. ¹H NMR (C₇D₈, 300 MHz): δ 7.20 (d, *J* = 7.8 Hz, 2H, H_o), 7.13 (t, *J* = 7.2 Hz, 2H, H_m), 7.00 (m, 2H, H_p), 6.54 (s, C_m-Mes-*H*), 3.40 (s, 2H, CH₂Ph), 2.16 (s, 6H, C_o-CH₃), 2.00 (s, 3H, C_p-CH₃), 1.13 (s, 54H, t, H_{bu}). ¹⁹F NMR (C₇D₈, 282 MHz): δ -123.1 (d, *J* = 22.0 Hz, 2F, F_o), -157.8 (t, *J* = 20.6 Hz, 1F, F_p), -160.2 (t, *J* = 20.6 Hz, 2F, F_m). ¹¹B NMR (C₇D₈, 96 MHz): δ -7.45. ¹³C{¹H} NMR (C₇D₈, 75 MHz): δ 135.5 (C_o of C≡N-Mes), 129.7 (C_o of CH₂Ph), 127.2 (C_m of CH₂Ph), 122.8 (C_p of CH₂Ph), 46.1 (C(CH₃)₃), 30.6 (C(CH₃)₃), 21.0 (*p*-CH₃), 18.5 (*o*-CH₃). ¹H NMR (C₆D₅Br, 300 MHz): δ 7.64 (d, *J* = 7.2 Hz, 2H, H_o), 7.46 (t, *J* = 7.2 Hz, 2H, H_m), 7.31 (t, *J* = 7.2 Hz, 2H, H_p), 7.11 (s, C_m-Mes-*H*), 3.83 (s, 2H, CH₂Ph), 2.69 (s, 6H, C_o-CH₃), 2.53 (s, 3H, C_p-CH₃), 1.63 (s, 54H, t, H_{bu}). ¹⁹F NMR (C₆D₅Br, 282 MHz): δ -128.5 (d, *J* = 22.0 Hz, 2F, F_o), -162.4 (t, *J* = 20.6 Hz, 1F, F_p), -165.0 (t, *J* = 20.6 Hz, 2F, F_m). ¹¹B NMR (C₆D₅Br, 96 MHz): δ -12.6. ¹³C{¹H} NMR (C₆D₅Br, 75 MHz): δ 202.3 (N=C), 150.1 and 147.0 (d, *J* = 232.5 Hz, C_{F-o}), 148.8 (C_{ipso} of CH₂Ph), 143.7 (C≡N), 139.1 and 135.9 (d, *J* = 240.0 Hz, C_{F-p}), 138.1 and 135.0 (d, *J* = 232.5 Hz, C_{F-m}), 135.5 (C_o of C≡N-Mes), 130.0 (C_{ipso} of C≡N-Mes), 129.6 (C_m of C≡N-Mes), 128.8 (C_o of CH₂Ph), 127.9 (C_m of CH₂Ph), 126.9 (C_p of C≡N-Mes), 122.5 (C_p of CH₂Ph), 45.8 (C(CH₃)₃), 30.3 (C(CH₃)₃), 21.0 (*p*-CH₃), 18.4 (*o*-CH₃).

Ti(N=C^{Bu})₃(η²-MeC≡N-Mes) (8). **5** (0.319 g, 0.66 mmol) was dissolved in toluene, and C≡NMe (0.10 g, 0.66 mmol), also dissolved in toluene, was added, at room temperature. An immediate deepening of the red color was observed. The mixture was stirred for 1 h at room temperature. The solvent was then removed and the residue extracted with hexane. Upon solvent removal a bright red solid was obtained (0.39 g, 96% yield). ¹H NMR (C₆D₆, 300 MHz): δ 6.79 (s, CH-Mes, 2H), 2.30 (s, CH₃, 3H), 2.14 (s, *p*-CH₃, 3H), 1.99 (s, *o*-CH₃, 6H), 1.31 (s, t, H_{bu}, 54H). ¹³C{¹H} NMR (C₆D₆, 75 MHz): δ 256.2 (C≡N-Mes), 184.6 (N=C), 145.0 (C_{ipso}), 134.3

Table 3. Crystallographic Data for **3** and **8**

	3	8
empirical formula	C ₅₄ H ₁₀₈ F ₁₁ N ₆ PTi ₃	C ₃₈ H ₆₈ N ₄ Ti
formula wt	1206.99	628.86
temp (K)	150(2)	150(2)
wavelength (Å)	0.710 69	0.710 73
cryst syst	monoclinic	monoclinic
space group	<i>P</i> 2 ₁ / <i>c</i>	<i>P</i> 2 ₁ / <i>n</i>
<i>a</i> (Å)	12.486(5)	11.7679(10)
<i>b</i> (Å)	13.689(5)	19.8939(18)
<i>c</i> (Å)	39.421(5)	17.5605(16)
α (deg)	90	90
β (deg)	92.643(5)	99.372(7)
γ (deg)	90	90
<i>V</i> (Å ³)	6731(4)	4056.2(6)
<i>Z</i>	4	4
<i>D</i> _c (g cm ⁻³)	1.191	1.030
abs coeff	0.437	0.238
<i>F</i> (000)	2544	1384
cryst size	0.1 × 0.1 × 0.4	0.2 × 0.2 × 0.3
cryst morphology	needle	block
color	green	red
θ range for data collec (deg)	2.47–23.45	3.29–23.25
limiting indices	-13 ≤ <i>h</i> ≤ 13 -15 ≤ <i>k</i> ≤ 15 -43 ≤ <i>l</i> ≤ 43	-6 ≤ <i>h</i> ≤ 13 -21 ≤ <i>k</i> ≤ 22 -19 ≤ <i>l</i> ≤ 17
no. of rflns collected/ unique (<i>R</i> _{int})	68 686/9451 (0.2165)	17 783/5666 (0.1023)
completeness to θ (%)	95.5 (θ = 23.45°)	97.4 (θ = 23.25°)
refinement method	full-matrix least squares on <i>F</i> ²	
no. of data/restraints/ params	9451/54/677	5666/0/392
goodness of fit on <i>F</i> ²	1.000	1.025
final <i>R</i> indices (<i>I</i> > 2σ(<i>I</i>))		
<i>R</i> ₁	0.0945	0.0960
<i>wR</i> ₂	0.2153	0.1947
<i>R</i> indices (all data)		
<i>R</i> ₁	0.1905	0.1195
<i>wR</i> ₂	0.2476	0.2138
extinction coeff	0.0332(19)	0
largest diff peak, hole (e Å ⁻³)	0.692, -0.386	0.515, -0.500

(C_o), 129.1 (C_p), 128.9 (C_m), 44.1 (C(CH₃)₃), 31.3 (C(CH₃)₃), 23.0 (CH₃), 20.9 (*p*-CH₃), 18.9 (*o*-CH₃). EI/FT ICR-MS: 628.48912 (100) ([C₃₈H₆₈N₄⁴⁸Ti]⁻). Anal. Calcd for C₃₈H₆₈N₄Ti: C, 72.58; H, 10.90; N, 8.91. Found: C, 69.25; H, 11.43; N, 8.35.

Ti(N=C^{Bu})₃(C₆F₅) (9). A solution of **1** (0.520 g, 1.03 mmol) in 40 mL of hexane was cooled to -50 °C, and a solution of C₆F₅-MgCl in ether (0.5 M, 1.14 mmol) was added. The mixture was warmed slowly to room temperature. After the mixture was stirred for 2 h at room temperature, the volatiles were removed and the residue was reextracted in hexane. Solvent removal gave 0.599 g of a bright red solid (91% yield). ¹H NMR (C₆D₆, 300 MHz): δ 1.21 (s, 54H, t, H_{bu}). ¹⁹F NMR (C₆D₆, 282 MHz): δ -112.2 (d, ³*J*_{F_oF_m} = 20.9 Hz, 2F, F_o), -154.8 (t, ³*J*_{F_pF_m} = 19.7 Hz, 1F, F_p), -160.8 (t, ³*J*_{F_mF_p} = 19.5 Hz, 2F, F_m). ¹³C{¹H} NMR (C₆D₆, 75 MHz): δ 199.5 (C≡N), 145.9 and 141.9 (d, *J*_{CF} = 300.0 Hz, C_o-F), 138.5 and 134.7 (d, *J*_{CF} = 285.0 Hz, C_p-F), 45.8 (C(CH₃)₃), 30.7 (C(CH₃)₃). ¹H NMR (C₇D₈, 300 MHz): δ 1.21 (s, 54H, t, H_{bu}). ¹⁹F NMR (C₇D₈, 282 MHz): δ -111.6 (m, 2F, F_o^A), -136.8 (m, 2F, F_o^B), -151.8 (t, *J* = 20.8 Hz, 1F, F_p^B), -154.1 (t, *J* = 19.5 Hz, 1F, F_p^A), -160.0 (m, 2F + 2F, F_m^A + F_m^B). ¹³C{¹H} NMR (C₇D₈, 75 MHz): δ 199.4 (C≡N), 45.8 (C(CH₃)₃), 30.7 (C(CH₃)₃). EI/FT ICR-MS: 635.315 17 (100) ([C₃₃H₅₄F₅N₃⁴⁸Ti]⁻).

General Procedures for X-ray Crystallography. Pertinent details for the individual compounds can be found in Table 3. Crystallographic data were collected using graphite-monochromated Mo Kα (λ = 0.710 73 Å) on a Bruker AXS-KAPPA APEX II area detector diffractometer equipped with an Oxford Cryosystem open-flow nitrogen cryostat, and data were collected at 150 K. Cell parameters were retrieved using Bruker SMART software and refined using Bruker SAINT on all observed reflections. Absorption

corrections were applied using SADABS. The structures were solved by direct methods using either SHELXS-97⁴⁵ or SIR 97⁴⁶ and refined using full-matrix least-squares refinement against F^2 using SHELXL-97.⁴⁷ All programs are included in the package of programs WINGX, version 1.64.05.⁴⁸ All non-hydrogen atoms were refined anisotropically, and the hydrogen atoms were inserted in idealized positions riding on the parent C atom. The molecular structures were done with ORTEP3 for Windows,⁴⁹ included in the software package.

Both crystals have low quality and poor diffracting power, which explain the low resolution, the small data to parameter ratio, and the high R values. Nevertheless, both structures were unequivocally determined and are in agreement with the remaining characterization data.

(45) Sheldrick, G. M. *Acta Crystallogr.* **1990**, *A46*, 467–473.

(46) Altomare, A.; Burla, M. C.; Camalli, M.; Casciaro, G. L.; Giacovazzo, C.; Guagliardi, A.; Moliterni, A. G. G.; Polidori, G.; Spagna, R. *J. Appl. Crystallogr.* **1999**, *32*, 115–119.

(47) Sheldrick, G. M. SHELXL-97, a Computer Program for the Refinement of Crystal Structures; University of Göttingen, Göttingen, Germany, 1997.

(48) Farrugia, L. J. *J. Appl. Crystallogr.* **1999**, *32*, 837–838.

(49) Farrugia, L. J. *J. Appl. Crystallogr.* **1997**, *30*, 565.

Data for complexes **3** and **9** were deposited with the CCDC under the deposit numbers 612083 and 612084, respectively, and can be obtained free of charge from the Cambridge Crystallographic Data Center, 12 Union Road, Cambridge CB2 1EZ, U.K. (tel +44 1223 336408, fax +44 1223 336033).

Acknowledgment. We thank Doctor M. Conceição Oliveira for EI/FT ICR-MS measurements. We are also grateful to the Fundação para a Ciência e Tecnologia for financial support (Projects POCTI/QUI/29734/2001 and POCTI/QUI/46206/2002). M.J.F. and I.M. are thankful for Ph.D. grants (BD2869/2000 and BD10338/2002, respectively) from the same institution and from the FSE.

Supporting Information Available: CIF files giving X-ray crystallographic data for compounds **3** and **8**, Figures S1–S23, giving NMR spectra of compounds **2–9**, Figure S24 giving the $\ln K$ vs $1/T$ plot for complex **9**, and Tables S1–S3, giving data for the $\ln K$ vs $1/T$ plot for **9**, the linear regression output, and regression statistics. This material is available free of charge via the Internet at <http://pubs.acs.org>.

OM060554W